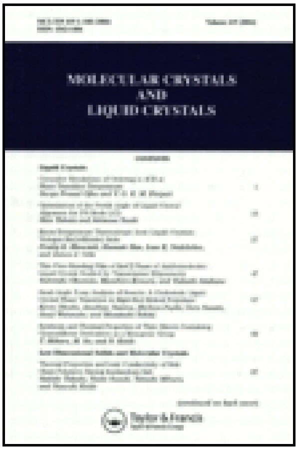

Molecular Crystals and Liquid Crystals
Publication details, including instructions for authors and subscription information:
http://www.tandfonline.com/loi/gmcl20

Devitrification of Bismuth Oxide Seal Frit for Back-Light Unit Lamp in LCD

Seong Jin Hwang [a], Yu Jin Kim [a], Mi Kyoung Park [a] & Hyung Sun Kim [a]
[a] School of Materials Engineering, Inha University, Incheon, Korea

To cite this article: Seong Jin Hwang, Yu Jin Kim, Mi Kyoung Park & Hyung Sun Kim (2007): Devitrification of Bismuth Oxide Seal Frit for Back-Light Unit Lamp in LCD, Molecular Crystals and Liquid Crystals, 470:1, 137-144

To link to this article: http://dx.doi.org/10.1080/15421400701493638

Mol. Cryst. Liq. Cryst., Vol. 470, pp. 137–144, 2007
Copyright © Taylor & Francis Group, LLC
ISSN: 1542-1406 print/1563-5287 online
DOI: 10.1080/15421400701493638

Devitrification of Bismuth Oxide Seal Frit for Back-Light Unit Lamp in LCD

Seong Jin Hwang
Yu Jin Kim
Mi Kyoung Park
Hyung Sun Kim
School of Materials Engineering, Inha University, Incheon, Korea

To replace the current PbO system of seal frits in the liquid crystal display (LCD) back-light unit (BLU), we examined the thermal behavior of lead-free frit, Bi_2O_3 *glasses. Frits consisting of a major composition of* Bi_2O_3, *ZnO and* B_2O_3 *were heat-treated and analyzed under different frit sizes using thermal analysis. The variation in frit size affected the crystallization mechanism of the frits during firing. Our findings suggest that devitrification of bismate glass frits is closely related to heating profile and frit size.*

Keywords: bismate glass; crystallization; liquid crystal display-back light unit; sealing

INTRODUCTION

An additional light source termed a back-light unit (BLU) is necessary for liquid crystal display (LCD) because of a non-emissive display. Current BLUs use straight fluorescent lamps as the light source, and recently a new design of flat fluorescent lamp (FFL) has been suggested that uses only one FFL by applying a driving circuit in the BLU for large-size LCD panels. The FFL BLU has the strong advantages of a bright source that reduces the total number of components in the present BLU and has also been in high demand due to both resource and environmental considerations [1,2].

This work is financially supported by the Ministry of Education and Human Resources Development (MOE), the Ministry of Commerce, Industry and Energy (MOCIE) and the Ministry of Labor (MOLAB) through the fostering project of the Lab of Excellency.

Address correspondence to Prof. Hyung Sun Kim, School of Materials Engineering, Inha University, Yonghyun-dong, Nam-gu, Incheon, 402-751, Korea (ROK). E-mail: kimhs@inha.ac.kr

Many researchers are actively studying the development of lead-free glass systems as an FFL seal [3,4]. Although the bismuth-containing sealing frit is an alternative solution to PbO frit, it has been reported to have a serious limitation in terms of microstructure: it crystallizes at a certain temperature near the firing condition [5,6]. If the glass seal is devitrified during firing, it encounters some problems of flowability and wetability, including the mismatch of the thermal expansion coefficient with a glass substrate, seriously degrading its performance as an FFL seal [7].

Our research aims to explain why the bismate glass is devitrified during firing. In this study, the Bi_2O_3-B_2O_3-ZnO glass system, one of the lead-free systems, is considered in terms of the thermal and physical properties of the glass. Our results demonstrate that the bismate glass frit is capable of preventing devitrification by controlling the glass frit size.

EXPERIMENTAL

The glass was prepared by mixing appropriate amounts of reagent grade Bi_2O_3, ZnO, H_3BO_3, $BaCO_3$ and Al_2O_3 powders. The batch was melted in an alumina crucible at 1000°C for 2 h. The glass melt was quickly poured and quenched on a ribbon roller. The glass cullet was pulverized by using a sieve (frit size$\leq$45 µm, $\leq$106 µm) and ball mill (frit size$\leq$10 µm). For the preparation of bulk specimens, the melts from the furnace were poured into a graphite mold and heated at 10°C above the glass transition temperature (T_g) of the glass for annealing.

The Littleton softening point (T_s) was measured on a thermal analyzer (SP-3A, Orton, USA). The T_g and onset point of crystallization (T_o) were determined by thermogravimetry – differential thermal analysis (TG-DTA, Rigaku, Japan) at a heating rate of 10°C/min with alumina as the reference. The frit was made from pellets (12.65 mm in diameter) by a uniaxial pressing method. Based on the DTA data of glass, each sample was heat-treated at 490°C $\sim$ 530°C at a heating rate of 10°C/min. The microstructure of the heat treated pellets was observed on a scanning electron microscope (SEM, HITACHI, Tokyo, Japan) on polished (0.25 µm diamond) and etched (5% nitric acid) surfaces. The fusion temperature of the frits was analyzed by a hot stage microscope (HSM, Ajeon, Korea), and the measurements were determined at an air heating rate of 10°C/min on cylinder-shaped samples of $\approx$3 mm height and $\approx$3 mm diameter. The samples were placed on $10 \times 10 \times 0.63$ mm alumina ($>$99.5%) supports.

RESULTS

The DTA results of glass in Figure 1 show an exothermal peak indicating a T_o similar to that of frits ($\leq 10\,\mu m$, $\leq 45\,\mu m$) as fine glass powder. However, no exothermal peak in the DTA result of the frit ($\leq 106\,\mu m$) as a bulk glass existed at an increased temperature of up to 600℃ heating. The T_g (370℃) was the same for all different frit sizes. The T_s ($\eta = 10^{7.6}$ dPa) of the glass was at 425℃. The T_g and T_s of the glass are originally thermal properties. However, as the glass frit shrinkage is related to the green density and tap density, the shrinkage behaviour should take the frit size into consideration.

The glass frit shrinkage ($\leq 10\,\mu m$, $\leq 45\,\mu m$, $\leq 106\,\mu m$) detected in HSM and the schematic model of glass sintering states are presented in Figures 2 and 3. The starting glass frit shrinkage ($\leq 10\,\mu m$), during the first state of glass sintering, was the fastest in all glass frits ($\leq 45\,\mu m$ and $\leq 106\,\mu m$), while the highest shrinkage stage was reached in the second state of the glass frit ($\leq 10\,\mu m$). At the third state of glass frit ($\leq 10\,\mu m$ and $\leq 45\,\mu m$), the rate of the shrinkage was almost the same, although that of glass frit ($\leq 106\,\mu m$) was greater than that of the other two glass frits. Moreover, the fourth state of glass frit ($\leq 106\,\mu m$) was reached before any crystal growth, according to the DTA result in which T_o did not exist in the glass frit ($\leq 106\,\mu m$).

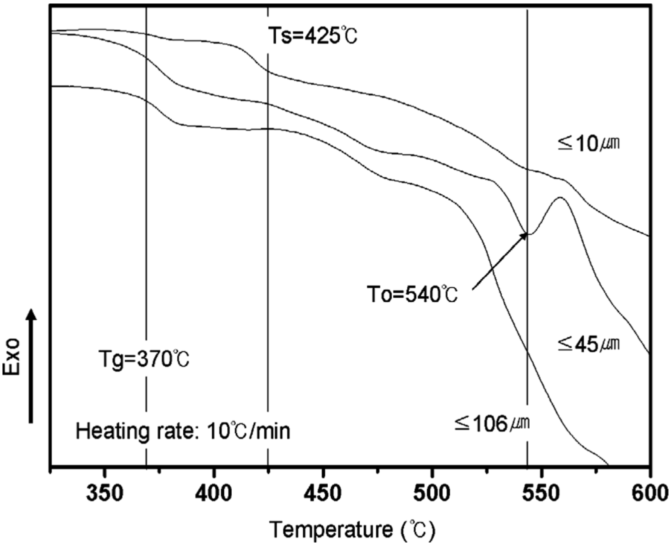

FIGURE 1 DTA non-isothermal curves of different frit size ($\leq 10\,\mu m$, $\leq 45\,\mu m$ and $\leq 106\,\mu m$).

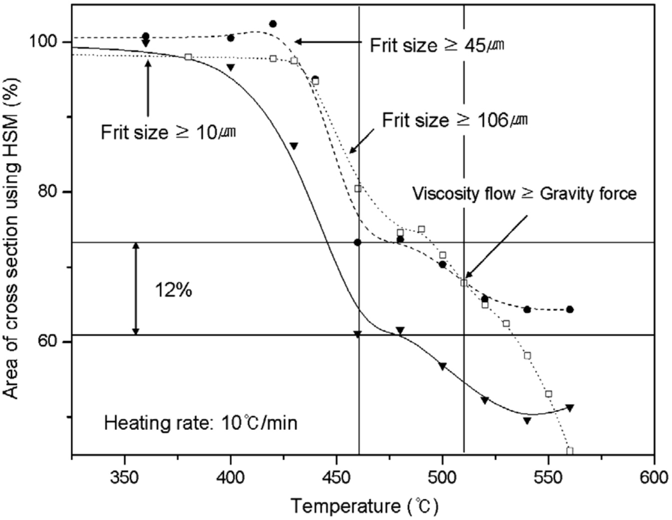

FIGURE 2 Changes in the cross sectional area of the pellet with different frits sizes (≤10 µm, ≤45 µm and ≤106 µm) during non-isothermal treatment.

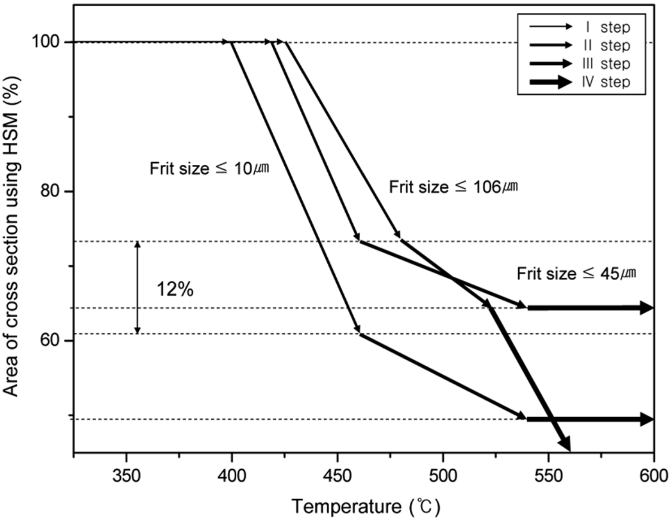

FIGURE 3 Schematic modeling of glass sintering states based on the changes in the cross sectional area using HSM for different frits sizes (≤10 µm, ≤45 µm and ≤106 µm).

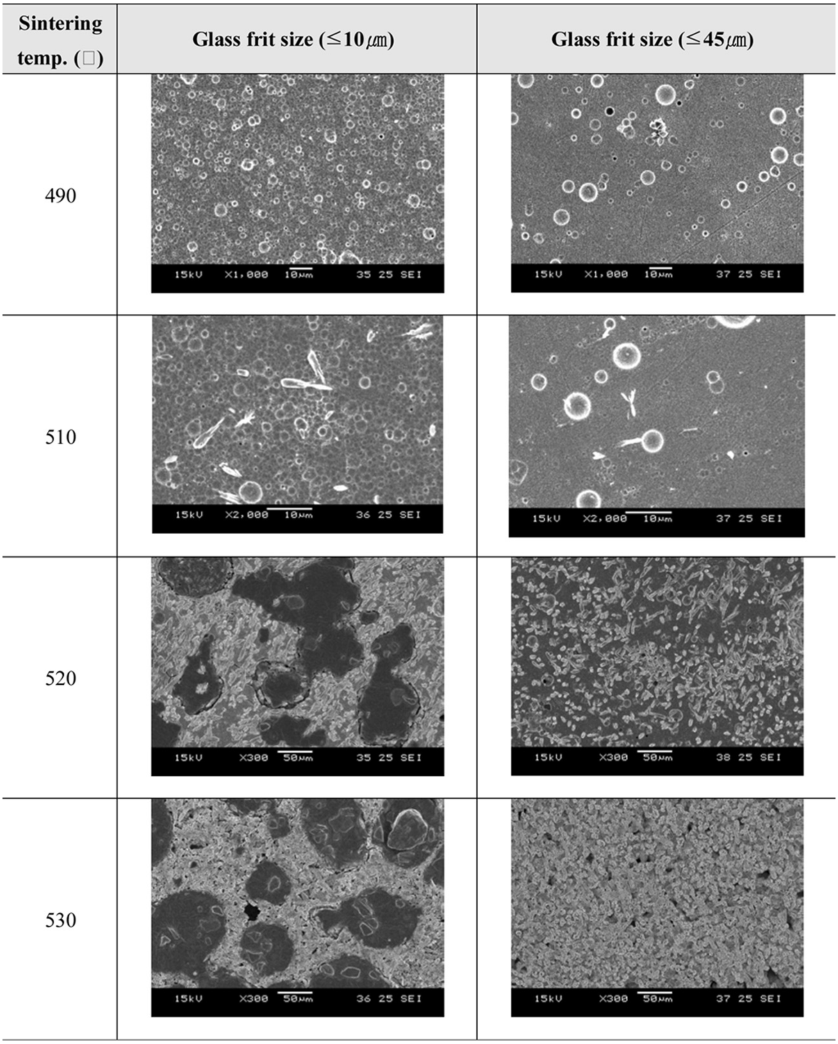

FIGURE 4 SEM images of heat treated samples as a function of temperature (490, 510, 520 and 530°C) with different frit sizes (≤10 µm and ≤45 µm).

We observed the changes in the cross sectional area of the sintered body as a function of temperature, as shown in Figure 4. The glass frits (≤10 µm and ≤45 µm) sintered at 490°C and 510°C were clearly amorphous. However, the glass frit (≤10 µm) sintered at 520°C was partially crystallized in the amorphous (dark regions) matrix, and a large amorphous region appeared in the sintered body. On the other hand, the crystal phase (white regions) showed homogeneously in glass matrix with the glass frit ($\leq 45\,\mu m$) sintered at 520°C. The morphologies were clearly shown with glass frit sintered at 530°C. The crystal (white regions) and amorphous (dark regions) phases were significantly separated in the sintered body with the glass frit ($\leq 10\,\mu m$) sintered at 530°C. The sintered body with the glass frit ($\leq 45\,\mu m$) sintered at 530°C was mostly covered with the crystal phase. There were amorphous regions, possibly consisting of glass clusters, in the sintered body of glass frit ($\leq 10\,\mu m$) sintered at 520 $\sim$ 530°C. Many pores formed by sintering with crystallization are evident in Figure 4. The pores from glass sintering were shaped as a regular circle, as shown in the sintered bodies of glass frit ($\leq 10\,\mu m$ and $\leq 45\,\mu m$) sintered at 490°C and 510°C. The irregularly shaped pores resulted from crystallization in the sintered body.

DISCUSSION

Considering that the fusion rate is faster than the crystal growth rate in glass sintering with the frit ($\leq 106\,\mu m$), crystal phases were absent in the sintered bodies, indicating that the glass had a viscosity low enough to interrupt crystal growth before the crystal phase formation. Furthermore, the viscosity flow of glass frit ($106\,\mu m$) sintered at 510°C overcame the gravity force. Consequently, the changes in the cross sectional area of the sintered body decreased dramatically (Fig. 2). However, crystallization of the glass resulted from bulk crystallization rather than from surface crystallization in the glass system, according to the DTA results which indicated that the exothermal onset temperature is the same as the other frits, irrespective of frit size (Fig. 1).

When the glass frits ($\leq 10\,\mu m$ and $\leq 45\,\mu m$) were sintered at the T_o of 540°C, the glass frit shrinkage was leveled by the crystal phase formation. The changes in the cross sectional area of the pellet are related to the glass viscosity and crystallization. The results shown in Figure 3 indicate that the glass sintering is composed of the four states: initial, shrinkage, viscosity flow, and crystallization or melt. The amorphous region existed mostly in the sintered body with glass frit ($\leq 10\,\mu m$ and $\leq 106\,\mu m$) sintered at 530°C. However, the sintered body of the glass frit sintered at 530°C was mainly composed of crystal phase. Thus, the changes in the cross sectional area of the pellet differed significantly among the different glass frit sizes. Further discussion on the formation of crystal phases in the sintered body will be reported in a future study because it is beyond the scope of this article.

A seal glass is normally sintered industrially with the heating profile shown in Figure 5. If the seal glass is crystallized during the

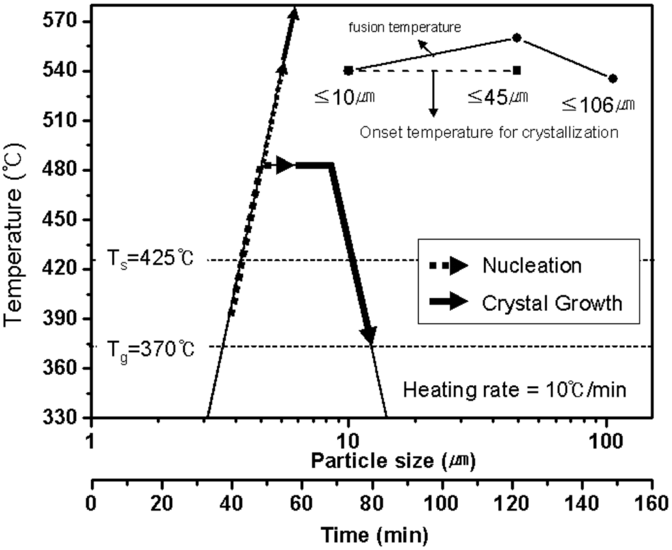

FIGURE 5 Heating profile of sealing for back-light unit lamp in LCD and a schematic model showing the relationship between crystallization (nucleation and crystal growth) and glass fusion temperature as a function of frit size.

heating profile, it undergoes two stages of nucleation and crystal growth, similar to that in a non-isothermal treatment. Thus, the glass frit may be considered in the non-isothermal treatment. The fusion temperature and T_o were nearly the same in the glass frit ($\leq 10\,\mu m$). Therefore, melt and crystallization occurred in the sintered body simultaneously at that temperature. However, the large frit size ($\leq 45\,\mu m$) crystallized before the fusion occurred. Crystallization occurs easily in a sintered body with glass frit ($\leq 45\,\mu m$), even if the glass frit ($\leq 10\,\mu m$) has more surface energy.

CONCLUSIONS

Analysis of the crystallization of the Bi_2O_3–B_2O_3–ZnO glass system with different frit sizes confirmed that the glass devitrification can be inhibited by controlling the frit size. With a smaller frit size, the fusion of frit occurred at a lower temperature and thus earlier in the firing time.

REFERENCES

[1] Kim, G. H. (2005). A PMMA composite as an optical diffuser in a liquid crystal display backlighting unit (BLU). *Eur. Polym. J.*, *41*, 1729.

[2] Chen, K. S., Wang, C. H., & Chen, H. T. (2006). A MAIC approach to TFT-LCD panel quality improvement. *Microelectornics Reliability*, *46*, 1189.

[3] Busio, M. & Steigelmann, O. (2000). New frit glasses for displays. *Glastech. Ber. Glass Sci. Technol.*, *73*, 319.

[4] Morena, R. J. (2000). Phosphate glasses as alternatives to Pb-based sealing frits. *Non-Cryst. Solids*, *263–264*, 382.

[5] Nitta, A., Koide, M., & Matusita, K. (2001). Glass formation and thermal properties of Bi_2O_3-ZnO-B_2O_3-R_2O quaternary systems. *Phys. Chem. Glasses*, *42*, 275.

[6] Zargarova, M. I. & Kasumova, M. F. (1990). Projection of the liquidus surface of the ZnO-Bi_2O_3-B_2O_3 system. *Inorganic Materials*, *26*, 1427.

[7] Kim, Y. J., Hwang, S. J., & Kim, H. S. (2006). Thermal properties of Bi_2O_3-B_2O_3-ZnO glass system. *Mat. Sci. Forum*, *510–511*, 578.